Journal Homepage: http://ijcpe.uobaghdad.edu.iq
Iraqi Journal of Chemical and Petroleum Engineering
Vol. 26 No. 3 (September 2025) 85 – 95
EISSN: 2618-0707, PISSN: 1997-4884

Utilizing red Iraqi kaolin for methylene blue sorption from aqueous solutions

Batool M. Saeed [a, b], Mohammed B. Abdul-Kareem [a, *]

a Department of Environmental Engineering, College of Engineering, University of Baghdad, Baghdad, Iraq
b Environmental Engineering Department, Mustansiriyah University, Baghdad, Iraq

Abstract

This paper explores the sorption potential of red Iraqi kaolin (IRK) for methylene blue (MB) elimination by sorption process. Batch tests were examined the impact of agitation time, IRK dose, pH, shaking speed, and MB concentration. The results demonstrated that IRK effectively removes MB, achieving a maximum elimination efficiency of 91.976% within 0.05 g/100 mL, 120 min, 7, 200 rpm and 50 mg/L for IRK dosage, contact duration, pH, shaking speed, and concentration of MB, respectively. The kinetic analysis showed that the sorption mechanism was fitted a pseudo 2nd order, therefore chemisorption is the primary mechanism. Intra-particle diffusion investigation demonstrated that the sorption mechanism is influenced by many concurrent procedures, particularly surface complexation and ion exchange. In addition, the Freundlich isotherm model fits the experiment's measurement higher than the Langmuir model, showing the heterogeneous surface features of IRK and the maximum sorption capacity (qmax) equal to 587.08 mg/g. The current investigation demonstrates the possibility of IRK as an effective and inexpensive sorbent for wastewater treatment applications, opening up opportunities for further research into sorbent regeneration and real-world wastewater situations.

Keywords: Methylene blue; Iraqi kaolin; sorption; wastewater treatment; kinetic modeling; and sorption isotherms.

Received on 15/11/2024, Received in Revised Form on 11/01/2025, Accepted on 12/01/2025, Published on 30/09/2025

https://doi.org/10.31699/IJCPE.2025.3.8

1- Introduction

With global population growth, the number of industrial manufacturing companies is expanding, leading to an increase in wastewater discharge into natural water bodies without adequate treatment. Industrial wastewater is often rich in organic compounds and is typically highly colored. Specifically, dye effluents contain toxic substances that significantly alter waterbody characteristics [1]. Methylene blue (MB) used in textiles, paper, rubber, plastics, and leather, as well as a staining agent in diagnostic and surgical operations. However, exposure to MB can pose health risks, including allergic dermatitis, eye irritation, and potentially mutagenic and carcinogenic effects [2]. Filtration [3], flotation [4], sorption [1, 3 - 6], and photocatalysis [7, 8] are some of the processes used for eliminating dyes from industrial effluent. Among them, sorption with solid materials is advised because it is simple, inexpensive, and easy to use [9, 10]. Numerous studies have explored MB sorption using affordable sorbents such as peanut stick wood [11], spent grated coconut [12], black cumin seed [13], fly ash [14], tea [15], black tea powder [16], and Ginkgo biloba leaves [17].

Kaolin, a clay mineral primarily composed of kaolinite is found extensively within the geological layers of Iraq's Western and Southern deserts, particularly as Iraqi red kaolin clay (IRK). It is most prevalent in mudrock formations ranging from the Ordovician to Cretaceous periods. Significant lithostratigraphic units containing IRK deposits include the Ga'ara Formation, the Hussainiyat Formation, and the Amij Formation, as well as smaller reserves of flint clay discovered at the base of the Hussainiyat Formation in karsts [18].

IRK has a broad range of technological applications, particularly as a promising sorbent. Its appeal lies in its low cost, eco-friendliness, and abundant availability. IRK from various regions has been studied for its effectiveness in removing diverse dyes from aqueous solutions, including methylene blue [19, 20], methyl orange [21] , malachite green [22] , and crystal violet [23]. Even though activated carbon is extremely efficient for dyes sorption, its high regeneration costs make it more costly than clay-based sorbents [24] The aim of this study is to investigate the sorption potential of red Iraqi kaolin (IRK) for the removal of methylene blue (MB) from aqueous solutions through the sorption process. Furthermore, evaluate the effectiveness of IRK as a sorbent for MB removal under various conditions and determine the optimal conditions for MB removal using IRK.

2- Materials and method

The IRK used in this study was obtained from the State Organization of Geological Survey and Mining in

*Corresponding Author: Email: m.mohamd@coeng.uobaghdad.edu.iq

Baghdad as Iraqi red kaolin (IRK) pieces from the Hussainiyat formation.

The rocks were washed with distilled water (DW) and heated in an oven at 90°C subsequently broken and sieved to generate solid particles ranging from 300 to 1000 µm. Methylene blue (MB) was utilized as the sorption test contaminant to prepare 1000 mg/L, one gram of dye powder was dissolved in one liter of DW.

2.1. Batch experiments

The sorption of MB by IRK was examined using batch studies under varied conditions. In these experiments, a specific quantity of IRK was added to 100 mL containing with 300 mg/L of MB and agitated with a shaker (Edmund Buhler SM25; Germany). For practical purposes, batch investigations have been conducted with different agitation intervals (0-180 min), pH levels (2-10), shaking speeds (0-350 rpm), and IRK doses (0.01-1.5 g per 100 mL). After the specified time duration, a fixed volume of 20 mL was extracted from each flask and centrifuged to separate the IRK from the solution. The MB concentration was determined with a UV-visible Model UV T80 at λmax = 665 nm.

The mass balance was utilized to compute the quantity of MB onto IRK, represented as qe (mg/g). [25]:

$$q_e = \frac{(C_o - C_e)V}{m} \quad (1)$$

Where q_e (mg/g) is the sorption capacity of MB per unit IRK dose, V (L) is the MB volume, C_o (mg/L) is MB initial concentrations and C_e (mg/L) is the MB equilibrium concentrations, and m (g) is the IRK dosage. Eq. 2 calculated the removal efficiency.

$$R\% = \frac{(C_o - C_e)}{C_o} \times 100 \quad (2)$$

2.2. Sorption isotherms

Sorption is often defined by isotherms, which indicate the equilibrium connection between the concentration of MB and the IRK particles at a certain temperature. This relationship is illustrated by a plot of the sorption capacity of MB per unit dose of IRK (q_e) vs the MB equilibrium concentration (C_e). To compare various materials, the amount is commonly standardized by the mass of the IRK [26]. In general, larger concentrations result in more adsorbed material per unit weight of IRK, but this increase is not strictly proportionate.

Convex upward isotherms consider advantageous because allow for comparatively high solid loading at low fluid contents. Concave upward isotherms, on the other hand, are regarded undesirable because they result in low solid loading and can form a protracted mass transfer zone inside the bed. The linear isotherm crosses the origin, suggesting that the amount of sorbed on IRK is proportional to its MB concentration in the fluid phase. These curves illustrate that sorption is a specific property that depends on the characteristics of the MB- IRK system. In the presence of a highly favorable isotherm, irreversible sorption occurs, which means that the amount of solute adsorbed stays constant regardless of concentration, even at extremely low levels [27]. The present investigation used two isotherm models, which are as follows:

1) Freundlich model: Primarily empirical and was eventually realized to reflect sorption on heterogeneous surfaces or ones with varied affinities. This model predicts that the most energetic sites are populated first, and that the site force decreases as additional sites are filled. The connection may be written as the following equation [28].

$$q_e = K_F C_e^{1/N} \qquad N > 1 \quad (3)$$

where K_F (mg/g) (l/mg)$^{1/N}$ is the Freundlich coefficient and N is an Freundlich empirical coefficient indicative of the intensity of the sorption.

2) Langmuir model: applies to single-layer sorption and assumes that maximal sorption occurs when a saturated monolayer of MB forms on the IRK surface. This model suggests that the sorption potential is constant and that no sorbate migrates inside the plane of the surface. [29].

$$q_e = \frac{q_m b C_e}{1 + b C_e} \quad (4)$$

where (q_m) is the maximum sorption capacity, and b is the Langmuir constant associated with the free energy.

2.3. Sorption kinetic study

Kinetics describes the rate at which a MB is sorbed, which determines the IRK residence duration at the IRK-MB interface. Understanding this kinetics is critical for determining the mechanics underlying the sorption process on diverse IRK. As a result, determining the amount of sorbate elimination from solutions is crucial for devising effective sorption treatment methods [30]. Two kinetic models were employed to examine the sorption mechanism and estimate the possible dominating phases:

1) Pseudo 1st order kinetic model: this model can be quantified by [31]:

$$\left(\frac{dq_t}{dt}\right) = K_1(q_e - q_t) = \pi r^2: \quad (5)$$

Where K_1 (min^{-1}) is the rate constant of pseudo 1st order, and q_t (mg/g) is the sorption quantity of MB sorbed at time t. Eq. 5 is integrated for the boundary conditions t = 0 to t = t and q_t = 0 to q_t = q_e. If the theoretical intercept (q_e) differs from the experimental intercept, the reaction cannot be first order, regardless of the coefficient of determination. The non-linear version of this model is given as follows:

$$q_t = q_e(1 - e^{-k_1 t}) \quad (6)$$

2) Pseudo (2nd order kinetic) model: Can be expressed as the equation below [32]:

$$\frac{dq}{dt} = k_2(q_e - q_t)^2 \quad (7)$$

K_2 (g.mg^{-1} min^{-1}) is the rate constant for pseudo 2nd order. Consider t=0 to t=t and q_t=0 to q_t=q_e. The non-linear form of Eq.7 is obtained by rearranging the integral form of Eq.8 [29, 33]:

$$q_t = \frac{t}{\left(\frac{1}{k_2 q_e^2} + \frac{t}{q_e}\right)} \quad (8)$$

3- Results and discussion

3.1. Characterization of IRK

The chemical and physical characterization of IRK were assessed through various analyses, including the chemical composition (by mass%) of IRK, which were analyzed using TruboQuant-Pellets X-ray fluorescence (XRF) at the Iraqi-German Lab at the University of Baghdad. As shown in Table 1, IRK is predominantly composed of alumina (Al_2O_3) at 21.78%, silica (SiO_2) at 46.47%, and ferric oxide (Fe_2O_3) at 15.01%. Additionally, several minor components such as MgO, CaO, Na_2O, K2O, TiO_2, ZrO_2, and P2O5 were detected in both materials, which may enhance the refractive index of kaolin.

XRD is used to analyze the crystalline characteristics of IRK, detecting crystals and crystalline characterization [34]. Fig. 1 shows the XRD patterns, with most peak locations remaining stable, showing that the underlying crystal structure has been conserved .

The surface appearance and microstructure of IRK were investigated using SEM. Fig. 1 demonstrates that IRK has a porous framework with a rough, uneven appearance and a range of block formations of varied sizes, despite its overall morphology being smooth with a few holes .[٣٥]

The EDS test is used to identify the elemental composition of IRK, as seen in Fig. 1 EDS analysis compares the observed X-ray intensity ratios generated by the elements in the material sample to those of a reference sample. The distinctive X-rays generated by each element are proportional to its concentration, likelihood of X-ray creation or ionization, and electron path length. This data is then compared to standard values to determine the composition of kaolin. Fig. 1 depicts the EDS spectrum data, showing the major elemental distribution, which includes peaks for oxygen, carbon, silicon, iron, and aluminum, all of which indicate an aluminosilicate structure.

Table 1. Oxide composition (%) for IRK determined by the XRF technique

Component	IRK (%)
SiO_2	46.47
Al_2O_3	21.78
Fe_2O_3	15.01
MgO	1.263
CaO	0.64
Na_2O	0.14
K_2O	1.22
TiO_2	2.25
ZrO_2	0.13
$P2O_5$	0.12
Loss on ignition (L.O.I)	10.72

Fig. 1 d shows the FTIR of IRK before and after MB sorption where at 1033 cm^{-1} has shifted to 1031 cm^{-1} due to the Si-O sorption MB while at 915 cm^{-1} has also shifted to 912 cm^{-1} because the Al-OH removes MB. The O-H stretching showed at 3694 cm-1, and vibration of coordinated water appear at 1640 cm-1. Moreover, a new band appeared at 1455 cm−1 due to the aromatic rings (C=C) of MB dye. The BET surface area and pore volume of IRK was obtained 71.49 (m²/g) and 0.06 cm3/g. This measurement indicates that the IRK has a high surface area compared to other clays such as Indian kaolin 13.69 m²/g, and Algerian kaolin 21.27 m²/g [36].

3.2. Operational conditions influence on sorption process

3.2.1. Agitation time

In batch studies, choosing an optimum contact time is critical to obtaining equilibrium concentrations. Fig. 2 shows how elimination efficiency changes with time duration at 0.05 g/100 mL of IRK dosage at 25ºC. The concentration of MB is 300 mg/L, the pH is 7, and the shaking speed is 200 rpm. The figures show a considerable increase in the proportion of pollutants removed as contact length rises. The sorption rate is initially high but progressively decreases with time, suggesting that the sorption sites on the sorbent surface have been saturated. After 120 min, almost 75.63% of the MB had been effectively removed. Beyond this time, the residual concentrations of these chemical species remained very constant, with only small fluctuations recorded close to 180 min.

The existence of several sites on the surface of IRK can explain the initial high rate of sorption, but the rate of reduction over time is most likely owing to MB's greater occupancy of these active sites. For instance, Luckham and Rossi (2024) found the removal efficiency occurs at 60 min, with equilibrium being reached shortly [37]. Research [38, 39] has shown kaolin can achieve higher adsorption capacities at shorter contact times for effective dye removal. Thus, a contact period of 120 min is judged adequate for future sorption tests since it approaches equilibrium.

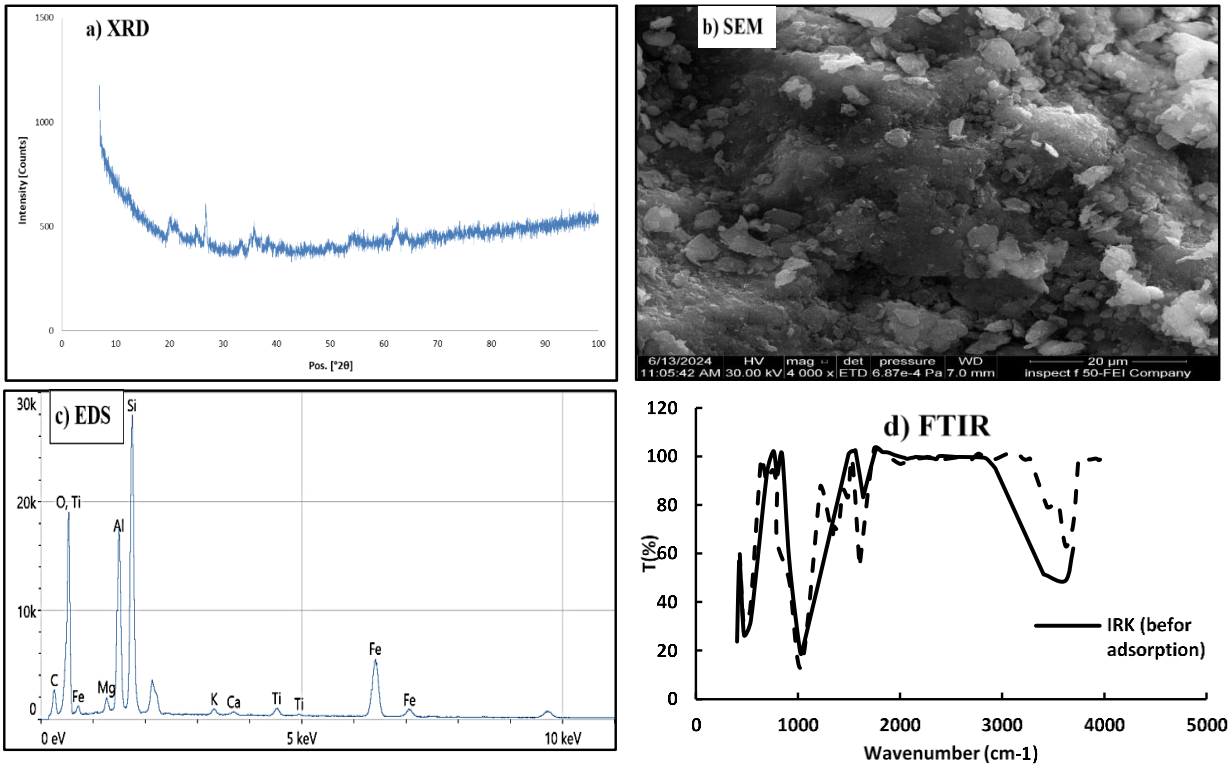

Fig. 1. XRD diffraction pattern (a), SEM (b), and EDS (c) FTIR (d) for IRK

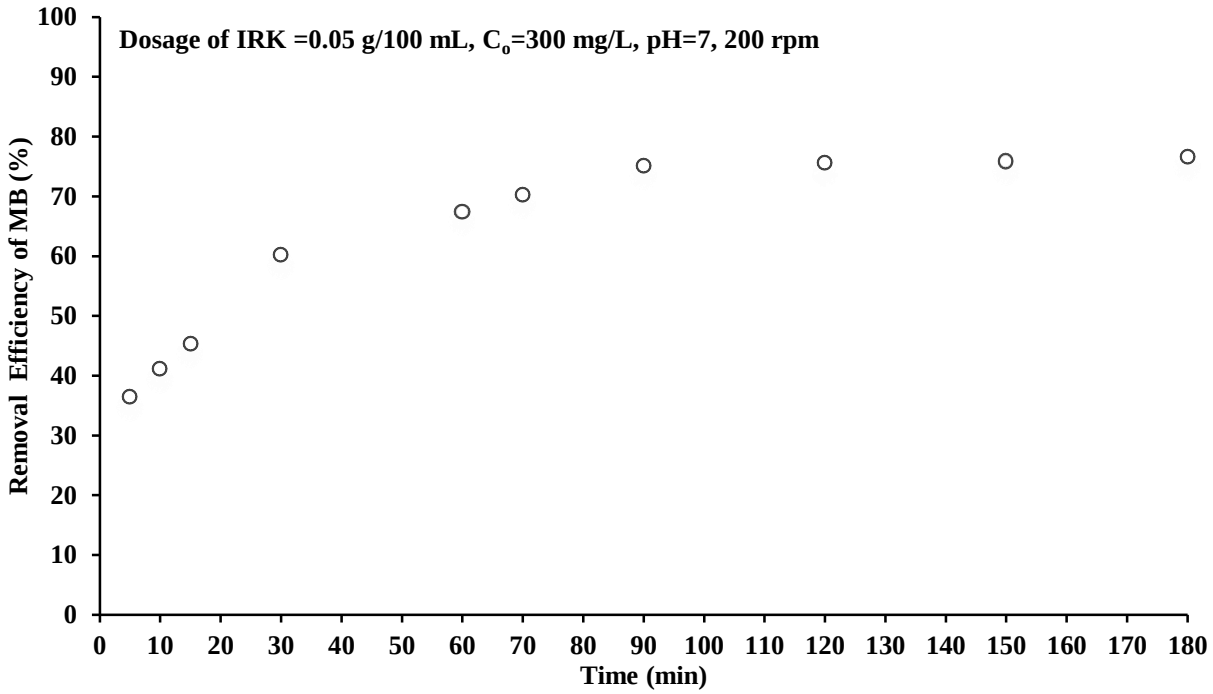

Fig. 2. Contact time effect on the elimination efficiency for MB on IRK (Dosage of IRK =0.05 g/100 mL, Co=300 mg/L, pH=7, 200 rpm)

3.2.2. IRK dosage

The impact of IRK dosage on sorption MB was investigated by testing various quantities of IRK (0.01 to 0.1 g). Each dose was continuously mixed with the MB solution (100 mL) under controlled parameters: temperature of 25ºC, concentration equal to 300 mg/L, pH of 5, shaking rate of 200 rpm, and time of agitation of 120 min. Fig. 3 demonstrates that the effectiveness of MB removal rises with greater dosages of IRK. This predicted tendency reflects the widely held belief that a higher volume of sorbent results in more potential active sites for sorption in solution. Kannan et al. (2001) noted that as the adsorbent dosage increased, the overall surface area available for adsorption also increased, leading to enhanced dye uptake [40].

3.2.3. Initial pH of MB

The influence of pH on the MB sorption onto IRK was examined at room temperature by different levels of pH of the. Fig. 4 demonstrates that elimination effectiveness improves as pH increases (2.0 to 10.0) at 300 mg/L ,120 min ,200 rpm for MB concentration, agitation time, and shaking rate, respectively. Higher pH levels were linked to higher MB sorption efficacy by IRK. This increase can be attributed to the electrostatic force between surface of IRK and MB, with maximal elimination occurring at pH 7 [41]. The point of zero charge for IRKC was determined to be 7 [36]; below this pH, the surface is positively charged and that leading to electrostatic repulsion with the cationic MB. On the other hand, the above that value, the surface is negative charges and resulting in strong electrostatic attraction.

3.2.4. Shaking speed

The influence of shaking speed on MB elimination effectiveness was examined by altering the agitation rate between 0 and 300 rpm while keeping all other parameters at the optimal values found in previous studies. Fig. 5 shows that with modest shaking, the elimination efficiency was around 34.75%, with increasing agitation rates resulting in a noticeable increase in MB removal. As the agitation rate was increased with the range 0 to 300 rpm, the elimination efficiency rose significantly, reaching around 80.8%. These findings suggest that greater agitation speeds promote the migration of MB to the surface of IRK. This increased diffusion results in improved sorption between the MB and surface of IRK, allowing for the efficient transfer of the MB to the IRK [42, 43].

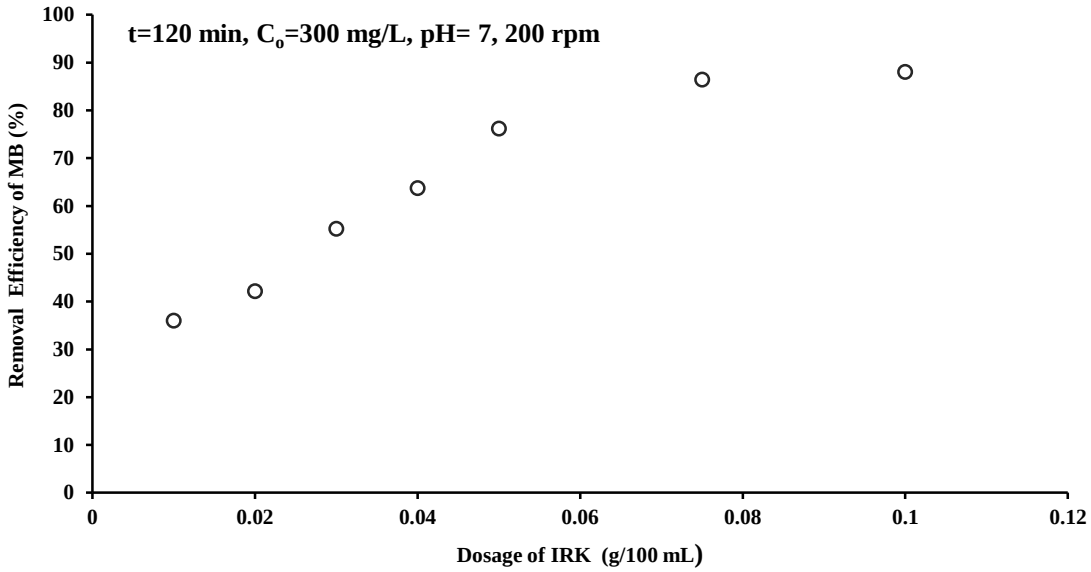

Fig. 3. The IRK dosage affects the effectiveness with which MB is removed from IRK (t=120 min, Co=300 mg/L, pH= 7, 200 rpm)

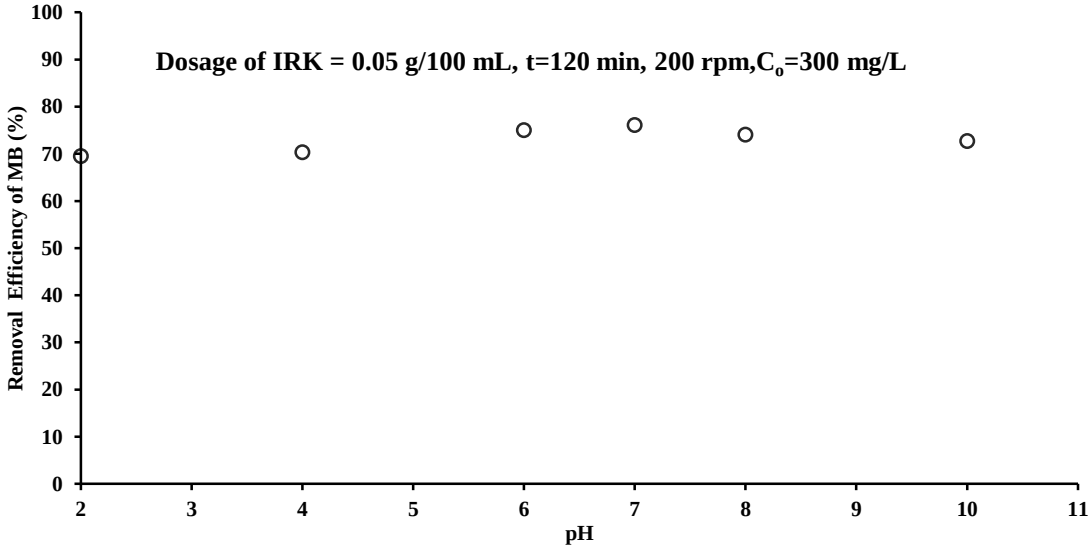

Fig. 4. Initial pH of MB effect on the elimination efficiency of MB (Dosage of IRK = 0.05 g/100 mL, t=120 min, 200 rpm, Co=300 mg/L)

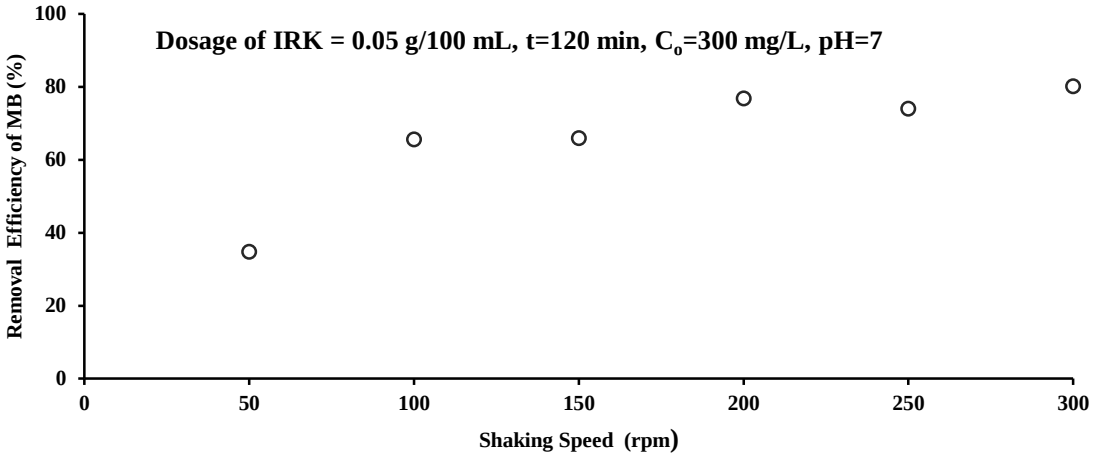

Fig. 5. Impact of shaking speed on the MB elimination percent (Dosage of IRK = 0.05 g/100 mL, t=120 min, Co=300 mg/L, pH=7)

3.2.5. MB initial concentration

Additional tests were examined to examine how different initial concentrations (C_o) of MB impact sorption efficacy. These tests used C_o levels (50 to 500 mg/L) with IRK dosage (0.05 g /100 mL) and shake for 120 min at shaking speed equal to 200 rpm, with an initial pH of 7. Fig. 6 shows how MB's elimination efficiencies changed with C_o at equilibrium. The results showed that elimination efficiencies were greater at lower C_o levels, but decreased as C_o increased, particularly more than 300 mg/L. This advancement can be related to the saturation of the IRK's MB-interacting sites. Furthermore, the results show a quick rise in the amount of MB adsorbed. Gupta et al. (2018) have been observed similar findings, where increased Co resulted in decreased elimination efficiencies due to the limited availability of active sites on the IRK [44].

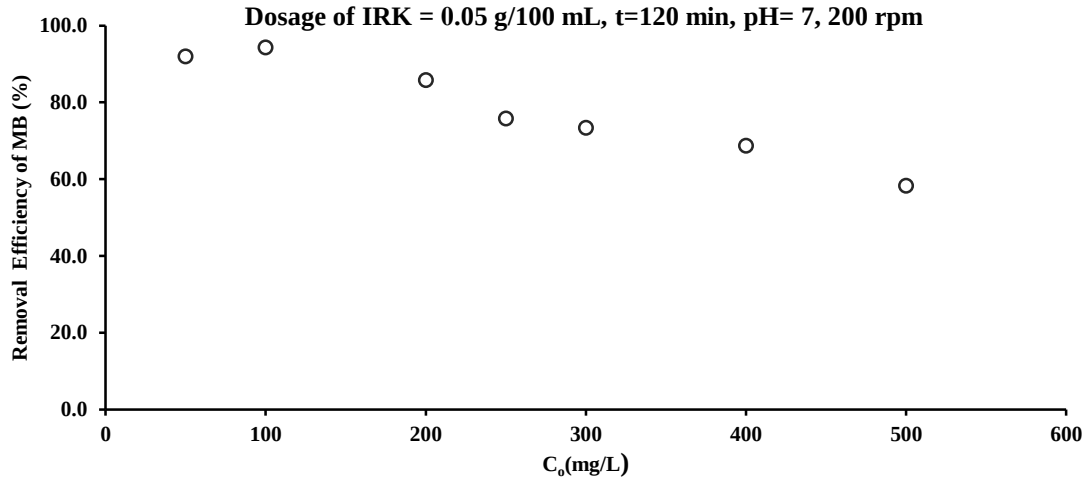

Fig. 6. Impact of MB concentration on elimination efficiency of MB (Dosage of IRK = 0.05 g/100 mL, t=120 min, pH= 7, 200 rpm)

3.3. Sorption kinetics

Sorption kinetics explains the rate at which MB is sorbed by sorbent particles, which analyses the time necessary to achieve equilibrium. Modeling the sorption kinetics allows us to determine the mechanisms that impact the transit of MB from the solution to the IRK. This simulation demonstrates that the sorption process is driven by reactions that occur on the surface of IRK. Designing successful treatment methods requires accurately calculating the sorption capacity of MB from the liquid phase [43, 45].

Fig. 7 displays the kinetic models fitted to the data collected through experiments for MB sorption on the surface. The solid line denotes the pseudo 1st order model, whereas the dotted line represents the pseudo 2nd order model. Table 2 lists the constants for these models, which were created using a fitting technique using Excel 2016's nonlinear regression "solver" function. The pseudo 2nd order model best fits the sorption process kinetics, with the greatest R^2 value and closest agreement between predicted and observed q_e values. This demonstrates that chemisorption is the primary mechanism at work, with valence forces driving the rate-limiting step of the

sorption mechanism by electron transfer or exchange between the sites of IRK and the MB [45].

Kinetic models alone cannot explain the mechanisms behind sorption processes. It is critical to integrate the intra-particle diffusion concept presented by Weber and Morris in 1962. This empirical model expresses the link between the quantity of adsorbed adsorbate and the square root of time ($t^{0.5}$), rather than time itself (t). The formula for this model is as follows:

$$q_t = k_{int} t^{0.5} + C \quad (9)$$

where, k_{int} is the rate constant for sorption in this model (mg/g $min^{0.5}$), and C is the intercept value that refers to the thickness of the boundary layer.

Fig. 7 shows a straight-line association between qt values and square root of time (t^0.5) for tested pollutants, with reasonably high R^2 values. However, these straight-line plots do not meet at the origin, showing that, while intra-particle diffusion plays a role in the sorption mechanism, it is not the rate-controlling step. Furthermore, the intra-particle diffusion plots show multi-linearity, indicating that MB sorption is controlled by two or more simultaneous processes [46]. The results indicate that surface complexation and ion exchange are the principal sorption processes, and that both the pseudo 2nd order and intra-particle diffusion kinetic models are valid.

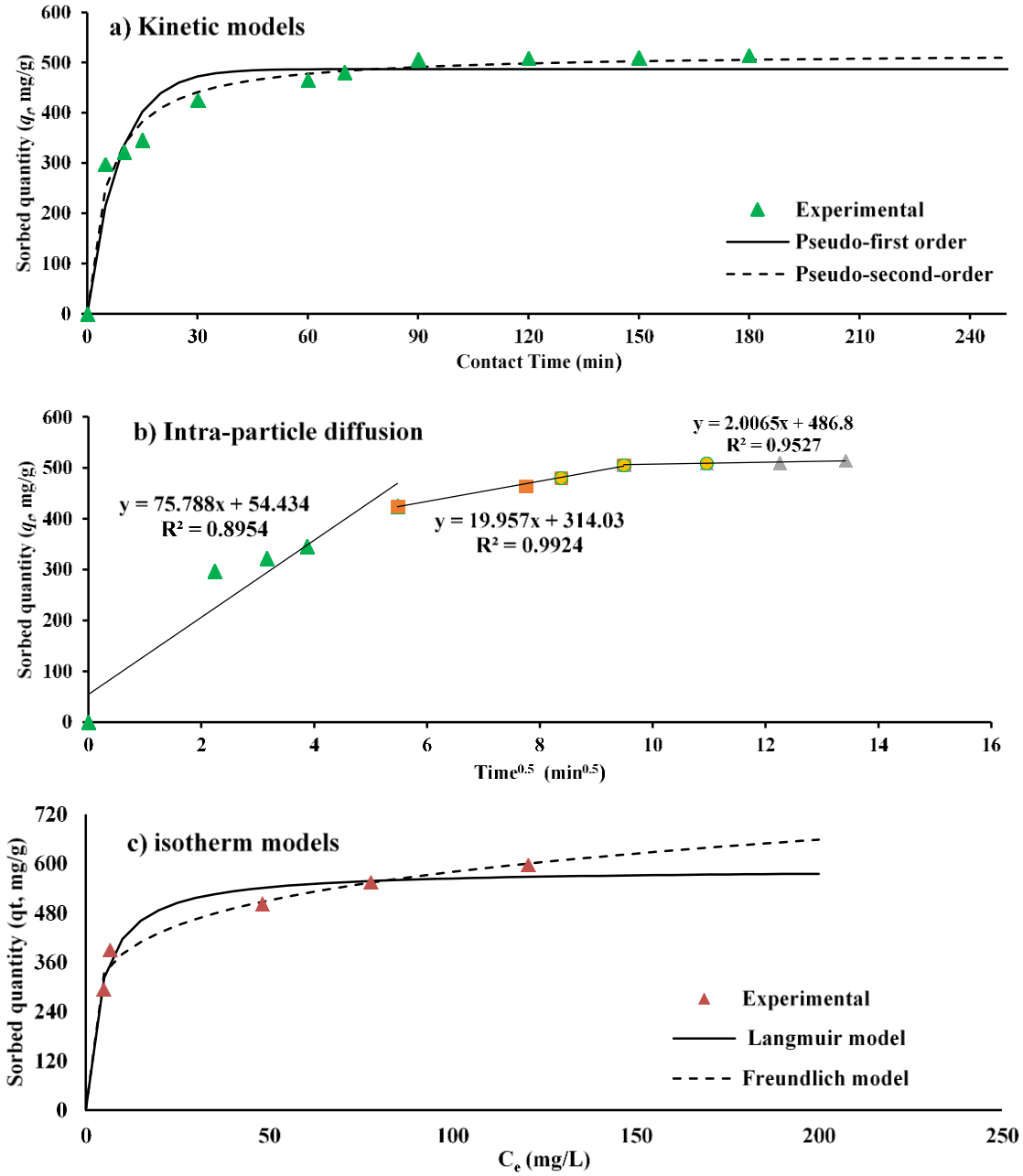

Fig. 7. Kinetic (a), Intra-particle diffusion (b), and isotherm models (c) compared with experiment results for a sorption of MB onto IRK

Table 2. Parameters of the kinetic models, intra-particle diffusion, and isotherm models for MB sorption onto IRK

Model	Parameter	Value
Freundlich	K_f (mg/g) (L/mg)$^{1/n}$	249.0363244
	n	5.451142424
	R^2	0.952816758
Langmuir	q_{max} (mg/g)	587.082646
	b (L/mg)	0.24347337
	R^2	0.94183691
Pseudo 1st order	q_e (mg/g)	486.8929624
	k_1 (1/min)	0.116223968
	R^2, SSE	0.940276891, 14972.82488
Pseudo 2nd order	q_e (mg/g)	520.6802537
	k_2 (g/mg min)	0.000352726
	R^2, SSE	0.98041607, 4733.99041
Intra-particle diffusion	Portion 1	
	k_{int} (mg/g min$^{0.5}$), C	75.788, 54.434
	R^2	0.8954
	Portion 2	
	k_{int} (mg/g min$^{0.5}$), C	19.957, 314.03
	R^2	0.9924
	Portion 3	
	k_{int} (mg/g min$^{0.5}$), C	2.0065, 486.8
	R^2	0.9527

3.4. Sorption isotherm models

The sorption isotherm displays the equilibrium distribution of MB through both liquid and solid phases throughout the sorption mechanism, as well as the maximum sorbent capacity and affinity. In this study, the Langmuir and Freundlich models were employed to fit the experimental data obtained from the synthesized sorbent, IRK. Throughout the experiments, mixing speed and duration were critical components of the preparation process. The sorption values were examined utilizing nonlinear regression by using the "solver" option in Excel 2016. The parameters for these models are listed in Table 2 The Freundlich model outperforms the Langmuir model in terms of R^2 and SSE.

4- Conclusions

This work evaluated the sorption properties of IRK for the elimination of MB from wastewater, indicating its substantial potential as an efficient sorbent, with up to 91.976% elimination efficiency achieved in 120 min. Operational characteristics such as sorbent dose, time, pH, shaking speed, and starting contaminant concentration all had an effect on elimination efficiency, with longer contact times and higher dosages improving elimination rates. Kinetic investigations revealed that the pseudo 2nd order model best describes the sorption process, implying that chemisorption is the dominant mechanism. Intra-particle diffusion study revealed the presence of many processes, the most important of which were surface complexation and ion exchange. Furthermore, the Freundlich model better reflected the sorption isotherm data than the Langmuir model, demonstrating the heterogeneity of the IRK surface. Overall, the work established IRK as a cost-effective sorbent for wastewater treatment, offering useful insights for building efficient sorption-based procedures. Future research will focus on enhancing sorbent regeneration and measuring performance in real-world wastewater settings.

References

[1] D. A. Yaseen and M.Scholz, “Textile dye wastewater characteristics and constituents of synthetic effluents : a critical review,” *International Journal of Environmental Science and Technology*, vol. 16, no. 2, pp. 1193–1226, 2019, https://doi.org/10.1007/s13762-018-2130-z

[2] G. Crini, G. Torri, E. Lichtfouse, G. Z. Kyzas, L. D. Wilson, and N. Morin-crini, “Dye removal by biosorption using cross-linked chitosan-based hydrogels,” *Environmental Chemistry Letters*, vol. 17, no. 4, pp. 1645–1666, 2019, https://doi.org/10.1007/s10311-019-00903-y

[3] S. Liu, Q. Wang, H. Ma, P. Huang, J. Li, and T. Kikuchi, “Effect of micro-bubbles on coagulation flotation process of dyeing wastewater,” *Separation and Purification Technology*, vol. 71, no. 3, pp. 337–346, Mar. 2010, https://doi.org/10.1016/j.seppur.2009.12.021

[4] G. L. Dotto *et al.*, “Development of chitosan/bentonite hybrid composite to remove hazardous anionic and cationic dyes from colored effluents,” *Journal of Environmental Chemical Engineering*, vol. 4, no. 3, pp. 3230–3239, Sep. 2016, https://doi.org/10.1016/j.jece.2016.07.004

[5] J. Georgin, G. L. Dotto, M. A. Mazutti, and E. L. Foletto, “Preparation of activated carbon from peanut shell by conventional pyrolysis and microwave irradiation-pyrolysis to remove organic dyes from aqueous solutions,” *Journal of Environmental Chemical Engineering*, vol. 4, no. 1, pp. 266–275, Mar. 2016, https://doi.org/10.1016/j.jece.2015.11.018

[6] R. Kant, “Textile dyeing industry an environmental hazard,” *Natural Science*, vol. 04, no. 01, pp. 22–26, 2012, https://doi.org/10.4236/ns.2012.41004

[7] E. da C. Severo, C. G. A. Anchieta, V. S. Foletto, and M. A. Kuhn, Raquel Cristine Collazzo, Gabriela Carvalho Mazutti, "Degradation of Amaranth azo dye in water by heterogeneous photo-Fenton process using FeWO 4 catalyst prepared by microwave irradiation," *Water Science and Technology*, pp. 88–94, 2016, https://doi.org/10.2166/wst.2015.469

[8] C. G. Anchieta *et al.*, "Rapid and facile preparation of zinc ferrite (ZnFe2O4) oxide by microwave-solvothermal technique and its catalytic activity in heterogeneous photo-Fenton reaction," *Materials Chemistry and Physics*, pp. 1–7, 2015, https://doi.org/10.1016/j.matchemphys.2015.04.016

[9] A. A. Atia, A. M. Donia, and W. A. Al-amrani, "Adsorption/desorption behavior of acid orange 10 on magnetic silica modified with amine groups," *Chemical Engineering Journal*, vol. 150, pp. 55–62, 2009, https://doi.org/10.1016/j.cej.2008.12.004

[10] Z. Salahshoor and A. Shahbazi, "Review of the use of mesoporous silicas for removing dye from textile wastewater," *European Journal of Environmental Sciences*, vol. 4, no. 2, pp. 116–130, Dec. 2014, https://doi.org/10.14712/23361964.2014.7

[11] M. Ghaedi, A. G. Nasab, S. Khodadoust, M. Rajabi, and S. Azizian, "Application of activated carbon as adsorbents for efficient removal of methylene blue: Kinetics and equilibrium study," *Journal of Industrial and Engineering Chemistry*, vol. 20, no. 4, pp. 2317–2324, Jul. 2014, https://doi.org/10.1016/j.jiec.2013.10.007

[12] K. Khalid, M. A. K. M. Hanafiah, and W. K. A. W. M. Khalir, "Effect of Physicochemical Parameters on Methylene Blue Adsorption by Sulfuric Acid Treated Spent Grated Coconut," *Applied Mechanics and Materials*, pp. 71–76, 2015, https://doi.org/10.4028/www.scientific.net/AMM.752-753.71

[13] S. I. Siddiqui, G. Rathi, and S. A. Chaudhry, "Acid washed black cumin seed powder preparation for adsorption of methylene blue dye from aqueous solution: Thermodynamic, kinetic and isotherm studies," *Journal of Molecular Liquids*, vol. 264, pp. 275–284, Aug. 2018, https://doi.org/10.1016/j.molliq.2018.05.065

[14] N. Yuan, H. Cai, T. Liu, Q. Huang, and X. Zhang, "Adsorptive removal of methylene blue from aqueous solution using coal fly ash-derived mesoporous silica material," *Adsorption Science and Technology*, vol. 37, no. 3–4, pp. 333–348, May 2019, https://doi.org/10.1177/0263617419827438

[15] T.-C. Lee *et al.*, "Tea stem as a sorbent for removal of methylene blue from aqueous phase," *Advances in Materials Science and Engineering*, vol. 2019, 2019, https://doi.org/10.1155/2019/9723763

[16] D. Lin *et al.*, "Adsorption of Dye by Waste Black Tea Powder: Parameters, Kinetic, Equilibrium, and Thermodynamic Studies," *Journal of Chemistry*, vol. 2020, 2020, https://doi.org/10.1155/2020/5431046

[17] R. Singh, T. S. Singh, J. O. Odiyo, J. A. Smith, and J. N. Edokpayi, "Evaluation of Methylene Blue Sorption onto Low-Cost Biosorbents: Equilibrium, Kinetics, and Thermodynamics," *Journal of Chemistry*, vol. 2020, 2020, https://doi.org/10.1155/2020/8318049

[18] M. Y.Tamar-Agha, M. A. A. Mahdi, and A. A. A. Ibrahim, "The Kaolin Clay Deposits in the Western Desert of Iraq: an Overeview," *Iraqi Bulletin of Geology and Mining*, no. 8, pp. 147–173, 2019.

[19] S. Ethaib and S. L. Zubaidi, "Removal of Methylene Blue Dye from Aqueous Solution Using Kaolin," in *IOP Conference Series: Materials Science and Engineering*, Iraq, 2020, p. 7. https://doi.org/10.1088/1757-899X/928/2/022030

[20] S. J. Olusegun, L. F. de Sousa Lima, and N. D. S. Mohallem, "Enhancement of adsorption capacity of clay through spray drying and surface modification process for wastewater treatment," *Chemical Engineering Journal*, vol. 334, pp. 1719–1728, Feb. 2018, https://doi.org/10.1016/j.cej.2017.11.084

[21] F. P. Sejie and M. S. Nadiye-tabbiruka, "Removal of Methyl Orange (MO) from Water by adsorption onto Modified Local Clay (Kaolinite)," *Physical Chemistry*, vol. 6, no. 2, pp. 39–48, 2016.

[22] N. Caponi, G. C. Collazzo, S. L. Jahn, G. L. Dotto, M. A. Mazutti, and E. L. Foletto, "Use of Brazilian Kaolin as a Potential Low-cost Adsorbent for the Removal of Malachite Green from Colored Effluents," in *Materials Research*, Universidade Federal de Sao Carlos, 2017, pp. 14–22. https://doi.org/10.1590/1980-5373-mr-2016-0673

[23] G. K. Sarma, S. S. Gupta, and K. G. Bhattacharyya, "Removal of hazardous basic dyes from aqueous solution by adsorption onto kaolinite and acid-treated kaolinite: kinetics, isotherm and mechanistic study," *SN Applied Sciences*, vol. 1, no. 3, Mar. 2019, https://doi.org/10.1007/s42452-019-0216-y

[24] Momina, M. Shahadat, and S. Isamil, "Regeneration performance of clay-based adsorbents for the removal of industrial dyes: A review," *Royal Society of Chemistry*, vol. 8, no. 43, pp. 24571-24587, 2018, https://doi.org/10.1039/c8ra04290j

[25] M. D. Mullassery, N. B. Fernandez, and T. S. Anirudhan, "Adsorptive removal of acid red from aqueous solutions by cationic surfactant-modified bentonite clay," *Desalination and Water Treatment*, vol. 56, no. 7, pp. 1929–1939, 2015, https://doi.org/10.1080/19443994.2014.958110

[26] G. Limousin, J. P. Gaudet, L. Charlet, S. Szenknect, V. Barthès, and M. Krimissa, "Sorption isotherms: A review on physical bases, modeling and measurement," *Applied Geochemistry*, vol. 22, pp. 249-275, 2007, https://doi.org/10.1016/j.apgeochem.2006.09.010

[27] A. A. H. Faisal, L. A. Naji, A. A. Chaudhary, and B. Saleh, "Removal of ammoniacal nitrogen from contaminated groundwater using waste foundry sand in the permeable reactive barrier," *Desalination and Water Treatment*, vol. 230, pp. 227–239, 2021, https://doi.org/10.5004/dwt.2021.27436

[28] A. A. H. Faisal and L. A. Naji, "Simulation of Ammonia Nitrogen Removal from Simulated Wastewater by Sorption onto Waste Foundry Sand Using Artificial Neural Network," *Association of Arab Universities Journal of Engineering Sciences*, vol. 26, pp. 28–34, 2019, https://doi.org/10.33261/jaaru.2019.26.1.004

[29] L. A. Naji, S. H. Jassam, M. J. Yaseen, A. A. H. Faisal, and N. Al-ansari, "Modification of Langmuir model for simulating initial pH and temperature effects on sorption process," *Separation Science and Technology*, vol. 0, no. 00, pp. 1–8, 2020, https://doi.org/10.1080/01496395.2019.1655055

[30] N. Saad, Z. T. A. Ali, L. A. Naji, A. A. A. H. Faisal, and N. Al-Ansari, "Development of Bi-Langmuir model on the sorption of cadmium onto waste foundry sand: Effects of initial pH and temperature," *Environmental Engineering Research*, vol. 25, no. 5, pp. 677–684, 2020, https://doi.org/10.4491/eer.2019.277

[31] M. T. Yagub, T. K. Sen, and H. M. Ang, "Equilibrium, kinetics, and thermodynamics of methylene blue adsorption by pine tree leaves," *Water, Air, and Soil Pollution*, vol. 223, 2012, https://doi.org/10.1007/s11270-012-1277-3

[32] E. Bulut, M. Özacar, and I. A. Şengil, "Equilibrium and kinetic data and process design for adsorption of Congo Red onto bentonite," *Journal of Hazardous Materials*, vol. 154, no. 1–3, pp. 613–622, 2008, https://doi.org/10.1016/j.jhazmat.2007.10.071

[33] Z. T. Abd Ali *et al.*, "Predominant mechanisms for the removal of nickel metal ion from aqueous solution using cement kiln dust," *Journal of Water Process Engineering*, vol. 33, no. September 2019, p. 101033, 2020, https://doi.org/10.1016/j.jwpe.2019.101033

[34] T. A. Aragaw and F. T. Angerasa, "Synthesis and characterization of Ethiopian kaolin for the removal of basic yellow (BY 28) dye from aqueous solution as a potential adsorbent," *Heliyon*, vol. 6, no. June, p. e04975, 2020, https://doi.org/10.1016/j.heliyon.2020.e04975

[35] Z. Huang *et al.*, "Modified bentonite adsorption of organic pollutants of dye wastewater," *Materials Chemistry and Physics*, vol. 202, pp. 266–276, 2017, https://doi.org/10.1016/j.matchemphys.2017.09.028

[36] A. H. Jawad and A. S. Abdulhameed, "Mesoporous Iraqi red kaolin clay as an efficient adsorbent for methylene blue dye: Adsorption kinetic, isotherm and mechanism study," *Surfaces and Interfaces*, p. 100422, 2020, https://doi.org/10.1016/j.surfin.2019.100422

[37] N. Hamri *et al.*, "Enhanced Adsorption Capacity of Methylene Blue Dye onto Kaolin through Acid Treatment: Batch Adsorption and Machine Learning Studies," *Water (Switzerland)*, vol. 16, no. 2, pp. 1–23, 2024, https://doi.org/10.3390/w16020243

[38] H. N. Hamad *et al.*, "Optimized Bentonite Clay Adsorbents for Methylene Blue Removal," *Processes*, vol. 12, no. 4, 2024, https://doi.org/10.3390/pr12040738

[39] C. P. Sagita, L. Nulandaya, and Y. S. Kurniawan, "Efficient and Low-Cost Removal of Methylene Blue using Activated Natural Kaolinite Material," *Journal of Multidisciplinary Applied Natural Science*, 2021, https://doi.org/10.47352/jmans.v1i2.80

[40] N. Kannan and M. M. Sundaram, "Kinetics and mechanism of removal of methylene blue by adsorption on various carbons - A comparative study," *Dyes and Pigments*, vol. 51, no. 1, pp. 25–40, 2001, https://doi.org/10.1016/S0143-7208(01)00056-0

[41] T. S. Anirudhan and M. Ramachandran, "Adsorptive removal of basic dyes from aqueous solutions by surfactant modified bentonite clay (organoclay): Kinetic and competitive adsorption isotherm," *Process Safety and Environmental Protection*, vol. 95, pp. 215–225, May 2015, https://doi.org/10.1016/j.psep.2015.03.003

[42] L. A. Naji, A. A. H. Faisal, H. M. Rashid, M. Naushad, and T. Ahamad, "Environmental remediation of synthetic leachate produced from sanitary landfills using low-cost composite sorbent," *Environmental Technology and Innovation*, vol. 18, p. 100680, 2020, https://doi.org/10.1016/j.eti.2020.100680

[43] M. Alshammari *et al.*, "Synthesis of a Novel Composite Sorbent Coated with Siderite Nanoparticles and its Application for Remediation of Water Contaminated with Congo Red Dye," *International Journal of Environmental Research*, vol. 14, no. 2, pp. 177–191, 2020, https://doi.org/10.1007/s41742-020-00245-6

[44] V. K. Gupta and Suhas, "Application of low-cost adsorbents for dye removal - A review," *Journal of Environmental Management*, vol. 90, no. 8, pp. 2313-2342, 2009, https://doi.org/10.1016/j.jenvman.2008.11.017

[45] Z. R. Komy, A. M. Shaker, S. E. M. Heggy, and M. E. A. El-Sayed, "Kinetic study for copper adsorption onto soil minerals in the absence and presence of humic acid," *Chemosphere*, vol. 99, pp. 117–124, Mar. 2014, https://doi.org/10.1016/j.chemosphere.2013.10.048

[46] W. H. Cheung, Y. S. Szeto, and G. McKay, "Intraparticle diffusion processes during acid dye adsorption onto chitosan," *Bioresource Technology*, vol. 98, no. 15, pp. 2897–2904, Nov. 2007, https://doi.org/10.1016/j.biortech.2006.09.045

استخدام طين الكاؤولين الاحمر العارقي لامتزاز صبغة ازرق المثلين من المحاليل المائية

بتول ماجد سعيد [١،٢]، محمد بهجت عبد الكريم [١،*]

١ جامعة بغداد، كلية الهندسة، قسم الهندسة البيئية، بغداد، العراق
٢ الجامعة المستنصرية، كلية الهندسة، قسم الهندسة البيئية، بغداد، العراق

الخلاصة

يستكشف هذا البحث إمكانية امتزاز طين الكاؤولين الأحمر العراقي (IRK) لصبغة ازرق الميثيلين (MB) من خلال تقنية الامتزاز. تم استخدام اختبارالدفعات لايجاد مدى تاثير بعض المتغيرات مثل وقت الخلط و كمية المادة المازة IRK و الدالة الهيدروجينية وسرعة الخلط وتركيز صبغة MB. أظهرت النتائج أن IRK يزيل MB بشكل فعال، محققًا أقصى كفاءة إزالة تبلغ ٩١,٩٧٦٪ في غضون ١٢٠ دقيقة باستخدام ٠,٠٥ غرام من المادة المازة / ١٠٠ مل ، عند رقم هيدروجيني ٧ و سرعة خلط ٢٠٠ دورة في الدقيقة بتركيز ٥٠ مليغرام / لتر من الصبغة الملوثة. وجد التحليل الحركي للبيانات أن نوذج (pseudo 2nd order) هو من مثل ميكانيكية الامتزاز، وبالتالي فإن الامتزاز الكيميائي هو الآلية الأساسية التي تم من خلالها عملية الازالة. أظهر تحقيق Intra-particle diffusion أن آلية الامتزاز تتأثر بالعديد من الإجراءات المتزامنة، وخاصة تكوين التعقيدات السطحية وتبادل الأيونات. بالإضافة إلى ذلك، فإن نموذج Freundlich ايزوثيرم يناسب مع القياسات التجريبية بشكل أعلى من نموذج Langmuir، مما يُظهر السمات السطحية غير المتجانسة لـ IRK مع اقصى سعة امتزازية (qmax) تساوي ٥٨٧,٠٨ مليغرام/غرام. يوضح البحث الحالي إمكانية استخدام IRK كممتز فعال وغير مكلف لتطبيقات معالجة المياه، مما يفتح فرصًا لمزيد من البحث في اعادة استخدام المادة المازة و استخدام الحالة الحقيقية لمياه الصرف الصحي في العالم.

الكلمات الدلة: صبغة ازرق المثلين، الكاؤولين العراقي، الامتزاز، معالجة المياه، النموذج الحركي، ايزوثيرم الامتصاص.